JAAS

Accepted Manuscript

This is an *Accepted Manuscript*, which has been through the Royal Society of Chemistry peer review process and has been accepted for publication.

Accepted Manuscripts are published online shortly after acceptance, before technical editing, formatting and proof reading. Using this free service, authors can make their results available to the community, in citable form, before we publish the edited article. We will replace this *Accepted Manuscript* with the edited and formatted *Advance Article* as soon as it is available.

You can find more information about *Accepted Manuscripts* in the Information for Authors.

Please note that technical editing may introduce minor changes to the text and/or graphics, which may alter content. The journal's standard Terms & Conditions and the Ethical guidelines still apply. In no event shall the Royal Society of Chemistry be held responsible for any errors or omissions in this *Accepted Manuscript* or any consequences arising from the use of any information it contains.

ROYAL SOCIETY OF CHEMISTRY

www.rsc.org/jaas

The quantitative measurement of trace elements in TiO_2 powders using a modified solution-cathode glow discharge–atomic emission spectrometry system has been developed.

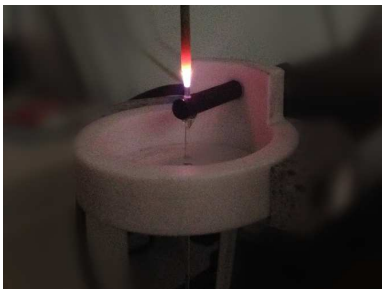

JAAS

RSCPublishing

ARTICLE

Design modification of a solution-cathode glow discharge–atomic emission spectrometer for the determination of trace metals in titanium dioxide

Zheng Wang,[a] * Rongyin Gai,[a,b] Lei Zhou[a,c] and Zhen Zhang[a]

Cite this: DOI: 10.1039/xoxxoooooox

Received ooth July 2014,
Accepted ooth July 2014

DOI: 10.1039/xoxxoooooox

www.rsc.org/

This paper describes the quantitative measurement of trace elements in TiO_2 powders using a modified solution-cathode glow discharge–atomic emission spectrometry (SCGD-AES) system. The optimal conditions utilized 0.1 M HNO_3 sample solutions and operated at a voltage of 1060 V with a flow rate of 2.0 mL min^{-1}. The TiO_2 matrix concentration tolerance of the SCGD source was determined to be 10 mg mL^{-1}. Sample solutions were prepared by dissolving different TiO_2 powders using a high temperature acid digestion method. The values determined by SCGD-AES are comparable to those obtained using axial inductively coupled plasma-atomic emission spectroscopy (ICP-AES). The proposed method was validated by quantifying Ag, Ca, Cu, Fe，K, Li, Mg，Na, and Pb in a certified reference material (NIST 154c), where the measurement results obtained by SCGD-AES agreed well with the reference values. In this method, Ti emissions were relatively weak, so that highly sensitive measurements of trace elements in TiO_2 matrices can be conducted with little interference. The detection limits of the trace elements such as Ag, Ca, Cu, Fe，K, Li, Mg, Na, and Pb in TiO_2 powders were 0.08, 2, 2, 5, 0.04, 0.02, 0.04, 0.02, and 0.4 μg g^{-1}, respectively. The enhancement of Pb sensitivity was also studied. Specifically, the limit of detection for Pb improved 6.5-fold to 2 ng mL^{-1} with the addition of 3% (v/v) formic acid.

1. Introduction

Titanium dioxide (TiO_2) is applied in various branches of modern industry and is utilized as a white pigment,[1–3] in cosmetics,[4–6] as a photocatalyst,[7–9] and in dye-sensitized solar cells.[10,11] Its physical and chemical properties can be significantly affected by metal impurities present at trace and ultra-trace levels. To obtain a TiO_2 pigment with good whitening ability, the concentration of discoloring impurities (*e.g.* Ca, Mg, Na, and Fe) must be reduced to commercially acceptable levels, as even minute concentrations of other metals can significantly impact whitening.[12] As a result of its extensive use in cosmetics, numerous international regulations limit the concentrations of elemental impurities in TiO_2. As a photocatalyst, TiO_2 has attracted much attention because of its applicability in the treatment of environmental wastes and pollutants. Ag ions, in combination with TiO_2, are known to enhance the inactivation of bacteria and repress their photoreactivation.[13] Notably, it was reported that as a photoelectrocatalyst with a controlled pore size, Fe doping improved the photocurrent density of TiO_2 samples.[14] Thus, for every particular application, the quality and purity of TiO_2 must be controlled to ensure product suitability. These effects highlight the necessity of an appropriate analytical method for the determination of trace impurities in TiO_2.

High-performance laboratory techniques such as inductively coupled plasma–atomic emission spectrometry (ICP-AES)[15,16] and inductively coupled plasma–mass spectrometry (ICP–MS)[17,18] have been used to determine trace amounts of impurities in TiO_2. However, these techniques consume large amounts of energy and are operated at high temperatures or under vacuum, and are thus impractical for portable measurement. Moreover, their operating costs are high and are therefore unsuitable for continuous monitoring. As titanium has a rich spectrum, many elements cannot be monitored well by ICP–AES because of spectral interference. To ensure rapid detection in a field measurement, it would be highly desirable to develop a more compact, low-cost instrument for on-site monitoring of metal ions.

Recently, different micro-plasma sources that perform well under many conditions have been developed.[19–32] Electrolyte-cathode discharge (ELCAD) has been investigated for more than two decades and has evolved considerably.[33–42] About ten years ago, solution-cathode glow discharge (SCGD) was described by Webb *et al.* as a simple configuration of ELCAD, and showed better performance than the parent system in

several studies.[43–46] The SCGD–AES method offers many advantages compared to ICP–AES/MS or atomic absorption spectroscopy (AAS): namely, its construction and operating costs are lower, it does not require plasma gas, fuel, or vacuum conditions, it does not need a nebulizer (which results in reduced memory effects and faster temporal response), it has lower power requirements, and it exhibits lower spectral interference.

Solution-electrode systems have been employed in several analytical applications. Acidified water[36,47–52] has occasionally been used as a sample solution for trace element analysis, but the analyte concentrations measured by ELCAD–AES were not compared to those determined by other techniques. Similarly, acid-diluted milk[53] was analyzed by ELCAD–AES, but the comparison to standard or certified reference materials was also lacking. Recent studies have reported the quantitative determination of trace elements in materials such as tuna fish, oyster tissue, coal fly ash,[54] zircaloys,[33] colloidal silica,[55] and environmental and biological samples.[56] The results agreed with the certified values. As the excitation temperature (measured using iron) in SCGD-AES (~5000 K)[46] is far lower than that in ICP-AES, Ti spectral lines are not excited. Thus, little spectral interference occurs in the monitoring of TiO_2 samples by SCGD-AES. In this work, the quantitative measurement of trace elements (Ag, Ca, Cu, Fe, K, Li, Mg, Na, and Pb) in TiO_2 using SCGD-AES was investigated and discussed. To the best of our knowledge, no studies focusing on the determination of TiO_2 powders using liquid-cathode glow discharge systems have been reported to date. Furthermore, there are no reports on the determination of numerous trace elements in a fast and convenient way that meets quality control analysis requirements.

2. Experimental

2.1. SCGD cell design

The SCGD cell used here was generally similar to the one used in former studies,[55,56] but was modified to improve its portability. In particular, the micropipette was directly connected to the graphite rod to remove the influence of the constant solution level. A photograph of the new design can be found in Fig. 1. A hole was drilled radially on one side of the graphite rod for insertion of the micropipette. The graphite rod passes horizontally through a hole drilled in one wall of the reservoir. The reservoir allows the pipette and graphite rod to be fixed. Sample solution enters the cell via a peristaltic pump through a 10 μL disposable micropipette (Fisher Scientific Co., Pittsburgh, PA) with a 1.1 mm outer diameter and an inner diameter of 0.38 mm. The distance between the top of the micropipette and graphite rod is 3 mm. The solution overflows from the tip connected with the grounded graphite electrode. A second glass pipette is positioned vertically in the waste reservoir to draw waste solution away. This arrangement is similar to the design of Doroski *et al.*,[57] but we retained the reservoir as a fixed device.

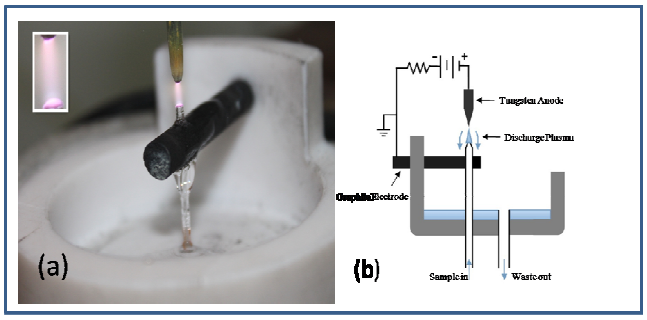

Fig. 1 Photograph (a) and schematic diagram (b) of the modified SCGD cell. (a) The main photo shows the discharge in the context of the new design cell and the inset (upper left) shows the discharge region only.

A two–channel peristaltic pump (Gilson, France) is used to pump sample solutions and carry waste solutions from the overflow reservoir. To reduce signal fluctuations induced by the pump, a simple and inexpensive custom-built pulse dampener is inserted between the pump and the SCGD. The dampener consists of a specially knotted (using a chain sinnet knot, also known as a daisy chain) length of peristaltic-pump tubing (two Tygon® tubes (with 1.52 mm inner diameter) joined to make a ~90 cm length before knotting).

The SCGD cell was mounted on a platform equipped with three orthogonal micrometer screw gauges, which could be adjusted precisely in the *x*, *y*, and *z* directions to produce the maximum signal and focus the discharge image onto the monochromator entrance slit. A Kepco (Flushing, NY) BHK 2000-0.1MG high-voltage power supply was used in constant voltage mode. To limit the discharge current, a 1.2 kΩ ballast resistor was introduced in series with the anode. The discharge was imaged at a magnification of 2.3:1 by a quartz lens positioned at the vertical entrance slit of the monochromator (Princeton Instruments, Action SP 2500, USA). A photomultiplier biased at 700 V was used as the detector. Emission spectra were recorded with an integration time of 0.015 s in 0.05 nm intervals. An Edmund Optics (Barrington, NJ, USA) GG 475 long-pass filter (greater than 88% transmission above 500 nm and less than 0.1% transmission below 460 nm) was used to block second-order emissions. SpectraSense v. 4.4.6 software (Princeton Instruments) was used to operate the spectrometer, control its configuration, and collect and process the data.

2.2 Reagents and samples

Deionized water (18.25 MΩ·cm resistivity) was obtained after passage through a water purification system (AWL-1002-U, Aquapro, China) in our laboratory. Working standards of the metals were prepared by appropriate dilution from the corresponding single-element 1000 μg mL^{-1} stock solutions. All sample solutions were acidified to pH 1.0 with HNO_3 (Sigma-Aldrich, ACS reagent, 65%). The pH of the solutions was measured with a pH meter (PHS-3E, INESA, China). Two TiO_2 powder samples (Aladdin Inc.), designated TiO_2-1 and TiO_2-2,

were used to study the applicability of the proposed method. A certified reference material (TiO_2 NIST 154c) was used to verify the accuracy of the SCGD-AES determinations. In addition, the following reagents were used: HCl (Tianjin Fengchuan Chemical Reagent Science and Technology Co., Ltd., GR), HF (Sinopharm Chemical Reagent Co., Ltd., GR), H_2SO_4 (Asia Union Electronic Chemical., Corp., GR), ammonium hydroxide (Sinopharm, AR), acetic acid (Sinopharm, AR), and formic acid (Sinopharm, GR).

2.3 Sample preparation for SCGD-AES and ICP-AES analyses

The TiO_2 sample or the certified reference material (TiO_2 NIST-154c) (~1.00 g) was weighed and dissolved in HF (5 mL) and HNO_3 (2 mL) in a PTFE vessel. The closed container was digested in an oven at 220°C for 16 h and then slowly cooled to room temperature slowly. The solution was transferred into a Pt crucible with deionized water and then evaporated to near-dryness on a heating platform. After transfer into a PET bottle with deionized water, the solution was diluted to 100 mL with deionized water and the pH was adjusted to 1.0 with ammonium hydroxide and HNO_3. The process blank was treated in the same way.

The process blanks and samples (both spiked and unspiked) were analyzed by the SCGD system in increasing analyte concentration in order to avoid issues caused by analyte carryover between samples. The SCGD was allowed to stabilize for 2 min prior to data acquisition. The monochromator scan speed was 200 nm min^{-1} and the data-sampling rate was 20 points per nanometer. Under these conditions, the integration time was 0.015 s. The digestion solutions were also measured using a Vista AX ICP-AES spectrometer with an axially viewed configuration (Varian, USA), and results were compared with the values measured by SCGD-AES.

3. Results and discussion

In this new SCGD system, preliminary studies to optimize several source parameters (electrolyte, flow rate, etc.) were carried out before the method was applied to real samples. These findings, along with other analytical characteristics, are described in more detail below.

3.1. Initial characterization and optimization

The analytical characteristics of the proposed technique were evaluated under preliminary conditions (electrode gap of 3.0 mm, slit width of 50 μm). The background emission spectrum of the SCGD was obtained using a solution of 0.1 M HNO_3, as shown in Fig. 2. Similar to most other solution-electrode discharges, the background spectrum was strong in several regions, particularly near the Mg I line at 285.2 nm. The most intense emissions were obtained from OH radicals, atomic hydrogen, atomic and ionic oxygen, and molecular nitrogen. Notably, the plasma was in contact with the tungsten electrode, but no tungsten lines were observed.

In contrast to the spectra obtained with previous SCGDs,[55,56] the emission of H_α and H_β was particularly strong. Bubbles were observed around the graphite rod during the discharge process. This may explain why the wave lines of H_α and H_β were noticeably increased compared to the earlier studies. In fact, although bubbles were observed in the initial study,[34] they were observed in a chamber that was separate from the discharge region. Even when the graphite rod was placed in the same chamber as the discharge region in the earlier studies, the bubbles were far removed from the plasma, so that they did not obviously affect the discharge.

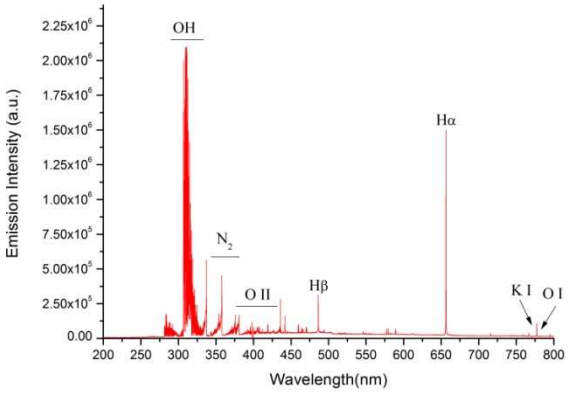

Fig. 2 Background spectrum (aqueous blank adjusted to pH 1.0 with HNO_3) of the SCGD-AES.

3.1.1. Acid selection

Standard solutions of Fe and Pb (10 μg mL^{-1} each) were prepared in three acids, including 0.1 M HNO_3, 0.1 M H_2SO_4, and 0.1 M HCl. The net intensities of Fe and Pb are shown in Fig. 3. The effects of the different acids were determined with the interelectrode gap, solution flow rate, and applied voltage held constant at 3.0 mm, 2.0 mL min^{-1}, and 1020 V, respectively.

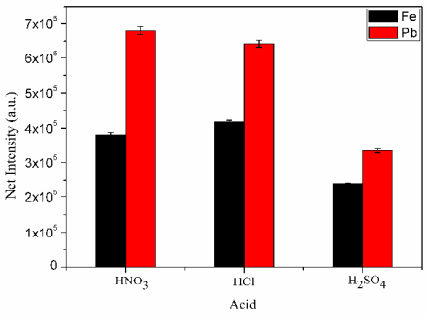

Fig. 3 The net intensities of 10 μg mL^{-1} Fe and 10 μg mL^{-1} Pb in 0.1 M HNO_3, 0.1 M H_2SO_4, and 0.1 M HCl. The solution flow rate, interelectrode gap, and discharge potential were held at 2.0 mL min^{-1}, 3.0 mm, and 1020 V, respectively.

Compared to H_2SO_4, HNO_3 and HCl exhibited higher net intensities for Fe and Pb. HNO_3 is a better electrolyte for the

detection of Pb, but HCl is more suitable for the detection of Fe. In our subsequent experiment, nitric acid was used for the preparation of the electrolyte solution. This is because nitric acid was more chemical compatibility for the determination of Ag in titanium dioxide samples, compared to the hydrochloric acid.

3.1.2. pH optimization

It is well known that SCGD/ELCAD is influenced by solution pH. During our experiments, it was found that the SCGD discharge strongly depended on the solution pH (adjusted with HNO_3). Figure 4 shows the effect of pH on the net emission intensities for Fe and Pb, which were determined from deionized water samples containing 10 μg mL^{-1} of Fe and Pb and detected at 248.32 and 405.78 nm, respectively. The net emission intensities increase as the pH increases from 0.6 to about 1.0, and they decreased as the pH increased from 1.0 to 1.6. The highest intensities for Pb and Fe were observed at pH 1.0. Notably, no other SCGD/ELCAD studies revealed decreased emissions at very low pH values. Below pH 0.6, the plasma is unstable, and above pH 1.6, the intensities were weaker. Therefore, it was determined that a stable plasma could be obtained between pH 0.6 and 1.6 and the highest Fe and Pb intensities could be obtained at pH 1.0. A similar trend was found for drop-spark discharges, which bear some similarities to ELCAD/SCGD.[40]

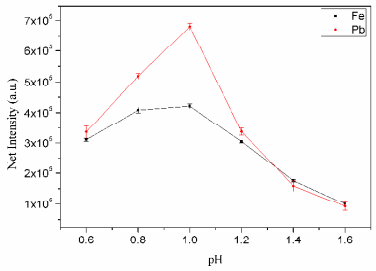

Fig. 4. The effect of acidity on the emission intensity for Fe and Pb. The solutions contained Fe or Pb (10 μg mL^{-1}) in HNO_3 at different pH. The solution flow rate and interelectrode gap were 2.0 mL min^{-1} and 3.0 mm, respectively. Emission lines: Fe (248.32 nm), Pb (405.78 nm).

3.1.3. Effect of applied voltage and solution flow rate

Based on the initial study, solutions of Fe and Pb (1.0 μg mL^{-1}) and the aqueous blank adjusted to pH 1.0 with HNO_3 were chosen as test samples to further investigate the characteristics of the SCGD system. To optimize emission signals and detection limits (DLs), the effects of the voltage and sample introduction flow rate on the Fe and Pb emission intensities were evaluated. The DL was defined according to the formula $DL = 3SD \times k^{-1}$, where SD is the standard deviation corresponding to 11 measurements of the blank samples and k is the slope of the calibration graph obtained from two points (solutions of Fe or Pb (1.0 μg mL^{-1}) and the aqueous blank adjusted to pH 1.0 with HNO_3). Multiple readings for each analyte solution and the acid blank solution were recorded. For the optimization studies, minimum DLs were designated as the analytical parameters to be evaluated.

Optimization of applied voltage An aqueous standard solution containing 1 μg mL^{-1} of Fe and Pb was used as a test sample to optimize the discharge performance of the SCGD system. First, a suitable applied potential was determined (Fig. 5a). In this test, the interelectrode gap was maintained at 3.0 mm and the solution flow rate was 2.0 mL min^{-1}. A continuous decrease in the DLs of Fe and Pb with voltages between 960 to 1060 V was found. However, the DLs began to level off at potentials ranging from 1060 to 1100 V. Minimal DLs were obtained at an applied potential of 1060 V (current, 67 mA; power, 71 W). Thus, an applied potential of 1060 V was used in the subsequent experiments.

Effect of solution flow rate With the electrode gap and applied voltage held constant at 3.0 mm and 1060 V, respectively, the influence of the sample-solution flow rate on the system performance was examined. The DLs decreased slightly with flow rates ranging from 1.4 to 2.0 mL min^{-1}, and subsequently increased slightly at flows ranging from 2.0 to 2.9 mL min^{-1} (Fig. 5b). The initial decrease in DLs with increasing flow rate may be attributed to the increasing amount of analyte entering the discharge. The slightly lower DLs at higher flow rates may be a consequence of additional water loading, which could reduce the energy in the discharge and minimize the effects of flow on the discharge gap. Because emissions were highest at 2.0 mL min^{-1}, this flow rate was chosen for subsequent experiments.

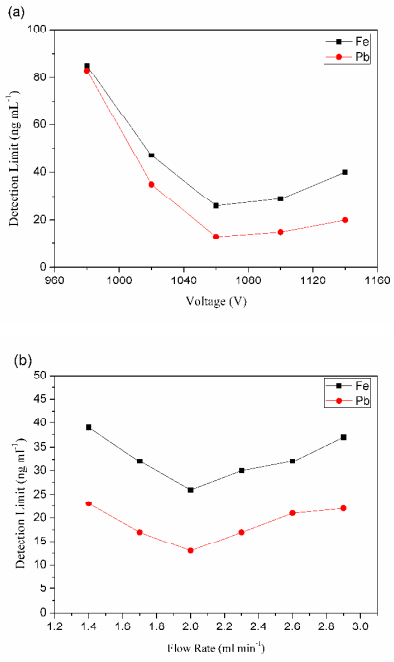

Fig. 5. Optimization of applied voltage (a) and solution flow rate (b). The electrode gap was held constant at 3.0 mm. Emission lines: Fe (248.32 nm), Pb (405.78 nm)

3.2. Analytical performance of modified SCGD design

The detection limits of Ag, Ca, Cu, Fe, K, Li, Mg, Na, and Pb by SCGD-AES are listed in Table 1. The DL is defined according to the formula DL = 3SD × k^{-1}, where SD is the standard deviation corresponding to 11 measurements of the blank samples and k is the slope of the calibration graph obtained from two points ((solutions of analyte (1.0 μg mL^{-1}) and the aqueous blank adjusted to pH 1.0 with HNO_3)). For comparison, the DLs from direct-current atmospheric-pressure glow discharge (dc-APGD), the earlier SCGD, ELCAD, and ICP-AES studies are also listed. Our instrument performed well compared to previously reported methods. The new SCGD cell design afforded almost the same DLs as those obtained in Webb's earlier SCGD work (essentially the best values reported to date). The advantages of the new design are the instrument's portability and rapid achievement of stability. The DLs for Li, Na, and K by SCGD-AES are much better than those obtained by ICP-AES, which highlights the potential of SCGD-AES as an alternative to ICP-AES in some instances.

Table 1 Comparison of detection limits (ng mL^{-1}) between present work and earlier studies

Element	Present Work[a]	dc-APGD[58]	SCGD[44]	ELCAD[33]	ICP-AES[59]
Ag	0.4	--	0.3	--	1
Ca	11	40	--	8	0.6
Cu	10	20	4	6	2
Fe	26	180	--	16	1
K	0.2	1.2	--	--	4
Li	0.08	0.3	0.06	--	1
Mg	0.2	8	0.2	5	0.3
Na	0.08	1	0.1	--	2
Pb	13	120	6	10	7

[a] Values obtained with the modified design.

3.3. Optimization of TiO_2 matrix tolerance for SCGD source stability

The concentration of the matrix usually has an effect on the accuracy of the determination in ICP-AES. It is not surprising that the matrix concentration may also affect determinations carried out by SCGD-AES.[46] The most important effect of the matrix is signal suppression, although it may result in signal enhancement or instability. In our initial experiment, the TiO_2 matrix suppressed the signals of metal impurities to a certain degree. Thus, to determine the metal impurities in TiO_2, the matrix tolerance must be established. Among the impurities, Pb and Fe, components of the TiO_2 sample, were selected for signal measurement. For the TiO_2 sample, a solution matrix (20 mg mL^{-1}) was first digested and then adjusted to pH 1.0. Solutions of different matrix concentrations (1, 2, 5, 10, and 15 mg mL^{-1}) were prepared by diluting the initial solution with 0.1 M HNO_3. The intensities of Pb and Fe in the TiO_2 solutions were monitored by SCGD-AES at the spectral lines of Pb I (405.78) nm, and Fe I (248.32) nm. The net signal intensities of the solutions containing different matrix concentrations are shown in Fig. 6. The net intensities did not vary in direct proportion to the matrix concentration, which suggests partial signal suppression. However, the percentage relative standard deviation values of the Pb and Fe signals did not change as much as the matrix concentrations increased. This means that the TiO_2 matrix did not noticeably affect the stability. The net signal for the matrix at 15 mg mL^{-1} was less than that at 10 mg mL^{-1}. However, below 10 mg mL^{-1}, the net signals showed a certain linearity as the matrix concentration increased. To accurately determine the net signals for metal impurities in TiO_2, a matrix concentration of 10 mg mL^{-1} was used in the following experiments and was considered the TiO_2 matrix tolerance of the SCGD source.

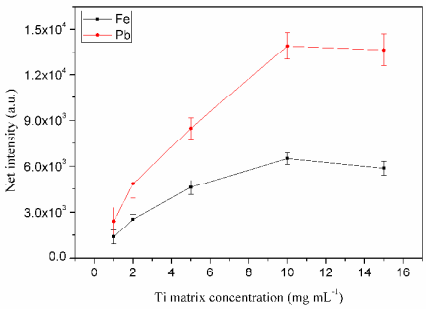

Fig. 6 Variation of net signals of Pb and Fe in different matrix concentrations of TiO_2 by SCGD-AES.

3.4. Determination of elemental impurities in TiO_2 powders

In the aforementioned experiment, we knew that matrix interference in the determination of metal impurities in TiO_2 typically appears as the suppression of emission intensity. This meant that the standard curve method would not be applicable in the determination of metal impurities in TiO_2. Hence, the standard addition method was used in the SCGD-AES and ICP-AES analyses.

A set of standard addition solutions with a matrix concentration of digested TiO_2 of 10 mg mL^{-1} was prepared in 0.1 M HNO_3. The corresponding blank solution was prepared in the same way. Two samples and TiO_2 NIST 154c were examined by SCGD-AES and ICP-AES. The samples were introduced into the SCGD cell at a flow rate of 2 mL min^{-1} and the emission signals for the trace elements were recorded. For Ag, Ca, Cu, Fe, K, Li, Mg, Na, and Pb, detection wavelengths of 328.06, 422.67, 324.75, 248.32, 766.49, 670.78, 285.21, 589.59, and 405.78 nm were used, respectively, for SCGD-AES. Many of the same wavelengths were used for ICP-AES with the exception of Fe, Mg, and Pb. For Fe, Mg, and Pb, more sensitive wavelengths and ion lines at 238.2, 279.6, and 220.4 nm were used, respectively. The results are listed in Tables 2 and 3. Pb, shown in Table 3, will be discussed in detail subsequently.

Spectral interference in ICP-AES influences the determination of many elements and often leads to worse DLs or precludes use of the optimal spectral line. When impurity

concentrations are near the DL, the values obtained by ICP-AES are sometimes inaccurate. Additionally, the high matrix concentration of Ti increases the background signal and deteriorates the DLs. As the excitation temperature (measured using iron) in SCGD-AES is about 5000 K,[46] most of the monitored spectral lines are atom lines, and most ion lines cannot be observed in the determination. Although the ion lines of Mg and a few other elements could be observed when highly concentrated standard solutions were used, the ion emission intensities were much lower than the atom lines. The optical emission spectrum has relatively few lines in SCGD-AES and there is little spectral interference from TiO_2 during element monitoring, which facilitates the determinations and enhances their accuracy. For example, the spectral lines at 328.068 and 338.289 nm, which are typically used in the determination of Ag by ICP-AES, are influenced by those of Ti at 327.999 and 338.377 nm; hence, the DL in ICP-AES is much worse for Ag. Because Ti spectral lines are not excited by SCGD-AES, the optimal line at 328.06 nm could be used in the determination of Ag. For the TiO_2 powders, the values obtained by SCGD-AES agree well with those obtained by ICP-AES. For the determination of elements in the standard TiO_2 NIST 154c, the values obtained by SCGD-AES and ICP-AES were close to the certified values, which indicated the reliability of SCGD-AES for this application. Li could not be detected in several samples due to its very low concentration. However, the DL of Li in SCGD-AES was much better than that by ICP-AES. Similarly, Pb could not be directly detected in the TiO_2 NIST 154c sample by either SCGD-AES or ICP-AES because of its low concentration.

Table 2 Comparison of SCGD-AES values (μg g^{-1}) with ICP-AES in TiO_2 powders (mean value ± SD (n = 5)).

	TiO_2-1		TiO_2-2	
Element	ICP-AES	SCGD-AES	ICP-AES	SCGD-AES
Ag	8 ± 0.6	9 ± 0.6	9 ± 0.7	11 ± 0.9
Ca	10 ± 1	8 ± 0.9	39 ± 3	34 ± 3
Cu	5 ±0.3	6 ± 0.4	8 ± 0.5	9 ± 0.5
Fe	38 ± 2	38 ± 3	30 ± 3	28 ± 2
K	2128 ± 142	1953 ± 135	2860 ± 197	2656 ± 185
Li	< 0.1	< 0.008	< 0.1	< 0.008
Mg	11 ± 0.7	12 ± 0.5	24 ± 2	26 ± 2
Na	16 ± 1	18 ± 1.0	19 ± 0.9	21 ± 1
Pb	25 ± 1	24 ± 1	36 ± 2	34 ± 2

Table 3 Comparison of SCGD-AES and ICP-AES values (μg g^{-1}) with the certified values in TiO2 NIST 154c (mean value ± SD (n = 5)).

Element	ICP-AES	SCGD-AES	Certified value
Ag	32 ± 2	30 ± 2	29
Ca	74 ± 5	72 ± 4	75
Cu	12 ± 1	11 ± 1	14
Fe	107 ± 9	113 ±7	100
K	32 ± 2	31 ± 2	31
Li	1.1±0.1	1.0± 0.1	0.9
Mg	16 ± 1	18 ± 2	17
Na	227 ± 18	238 ± 24	220
Pb[a]	<3	0.9 ± 0.1	1.1

[a] The values of Pb obtained in SCGD-AES is measured with the enhancement of formic acid (3%, v/v).

3.5. Study of SCGD-AES sensitivity enhancement for Pb

Although the signals were suppressed, the net intensities of most elements of interest could be recorded with the exception of Pb; its low concentration in TiO_2 NIST 154c precluded its direct detection. The quantification of Pb in TiO_2 is a significant problem that can be solved by improving the sensitivity of the method. Formic acid was shown to enhance sensitivity for Pb in earlier studies,[33,60,61] and other reagents such as cetyltrimethylammonium chloride,[56] Triton X-405,[58] and CH_3COOH[60,61] have been similarly applied for other elements. As HCOOH improved sensitivity toward Pb, HCOOH and its homologue CH_3COOH were chosen to enhance Pb sensitivity in the following studies.

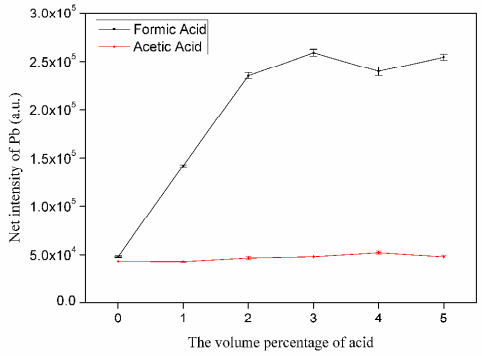

Fig. 7 Variation of net signal of element Pb with different volume ratios of formic acid and acetic acid.

Solutions of Pb (1 μg mL^{-1}) with different formic acid contents (0, 1, 2, 3, 4, and 5 vol%) in 0.1 M HNO_3 and the corresponding blank solutions were prepared. Solutions using acetic acid were prepared in a similar fashion. The addition of formic acid enhanced the emission intensities dramatically, and the best enhancement was acquired when the formic acid content was 3 vol%. In contrast, the emission intensities did not change significantly with the solutions containing acetic acid. With the formic acid enhancement, the best Pb detection limit was 2 ng mL^{-1}, which was far below the concentration of Pb in the digested solutions of TiO_2 NIST-154c. Enhancement by acetic acid was not obvious for the standard or the corresponding blank solutions. The Pb detection limit was improved 6.5 times in the presence of 3 vol% formic acid over that in its absence. Thus, the addition of formic acid was confirmed as an effective method to enhance the detection of Pb. With this approach, the Pb content in TiO_2 NIST 154c could be detected accurately, giving a value that was in accord with the certified value. The Pb concentration was so low that it could not be detected by ICP-AES. The Pb value shown in Tables 3 was obtained in the presence of 3 vol% formic acid.

The mechanism behind the Pb signal enhancement is not clearly understood. In earlier studies, different reagents were

used to enhance the emission intensities of many elements, and the mechanism was variously explained.[33,56,58,60,62] Some believed that the effects are related to changes in the solution characteristics, such as surface tension.[56,60,62] As the sputtering of dissolved metal ions from the surface of an electrolyte solution may be enhanced by a reduction of surface tension, the sample introduction efficiency may be improved. At the same time, changes in the excitation temperature, ion density, and other discharge characteristics may enhance the emission intensity observed from the plasma discharge. Notably, the background did not obviously change. As the background fluctuation was similar to that without the addition of formic acid and the sensitivity improved after the addition of formic acid, the DL improved from 13 ng mL^{-1} to 2 ng mL^{-1}. The addition of acetic acid may not obviously change the properties, thus accounting for its poor performance in the enhancement of the emission intensity of Pb. Further exploration of these ideas will be reported in due course.

3.6. Limits of detection for TiO_2 powders determination

Although the background spectrum did not change significantly, the actual DLs worsened to some degree for many elements when monitored in TiO_2 powders, primarily because the emission intensities were suppressed when the matrix concentration was not low enough. The matrix concentration used in this study (10 mg mL^{-1}) avoided over dilution of the monitored elements and did not excessively suppress their emission intensities. The DLs did not change significantly for most elements, and the DLs for all monitored elements were not more than twice those without the TiO_2 matrix. Thus, the DLs for Ag, Ca, Cu, Fe, K, Li, Mg, Na, and Pb in the TiO_2 powders were 0.08, 2, 2, 5, 0.04, 0.02, 0.04, 0.02, and 0.4 μg g^{-1}, respectively.

4. Conclusions

The modified SCGD design showed good performance with low limits of detection, and has greater portability as compared to earlier SCGD or ELCAD instruments. With the addition of formic acid (3 vol%), the Pb DL was improved to 2 ng mL^{-1}, which was much lower than the DL without the additive.

SCGD-AES is a useful method for the determination of metal impurities in TiO_2, as it has a much lower power usage and does not require noble gases. It exhibits less spectral interference than ICP-AES. By comparing the values obtained in SCGD-AES with the certified values for TiO_2 NIST-154c, the determinations of trace levels of Ag, Ca, Cu, Fe, K, Li, Mg, Na, and Pb in TiO_2 were proven to be accurate and reliable. The SCGD-AES analytical method was shown to be a viable alternative for the determination of elements in a complex sample matrix, and it showed good potential for the measurement of trace levels of metal impurities in other ceramics materials.

Acknowledgements

This work was financed by a program of the Shanghai Science and Technology Commission through Grant No. 12142200200.

Notes and references

[a]*Shanghai Institute of Ceramics, Chinese Academy of Science, Shanghai, 200050*
[b]*School of Chemical Engineering, Changchun University of Technology, 130012*
[c]*School of Materials Science and Engineering, Donghua University, Shanghai 201620*
[*]*Corresponding author: Fax: (+86)21-52413016; E-mail: wangzheng@mail.sic.ac.cn*

1 P. S. Croce and A. Mousavi, *Environ Chem Lett*, 2013, **11**, 325-328.
2 K. J. Park, K. U. Lee, M. H. Kim, O. J. Kwon and J. J. Kim, *Curr App Phys*, 2013, **13**, 1231-1236.
3 C. X. Tian, S. H. Huang and Y. Yang, *Dyes Pigments*, 2013, **96**, 609-613.
4 C. Y. Su, H. Z. Tang, K. Chu and C. K. Lin, *Ceram. Int.*, 2014, **40**, 6903-6911.
5 A. Jaroenworaluck, W. Sunsaneeyametha, N. Kosachan and R. Stevens, *Surf. Interface Anal*, 2006, **38**, 473-477.
6 H. H. Ko, H. T. Chen, F. L. Yen, W. C. Lu, C. W. Kuo and M. C. Wang, *Int. J. Mol. Sci*, 2012, **13**, 1658-1669.
7 J. Lu, L. H. Li, Z. S. Wang, B. Wen and J. L. Cao, *Mater. Lett.*, 2013, **94**, 147-149.
8 A. K. L. Sajjad, S. Shamaila and J. L. Zhang, *Mater. Res. Bull.,* 2012, **47**, 3038-3089.
9 S. D. Sharma, D. Singh, K. K. Saini, C. Kant, V.Sharma, S. C. Jain and C. P. Sharma, *Appl. Catal., A* , 2006, **314**, 40-46.
10 M. H. Abdullah and M. Rusop, *J. Alloys Compd.*, 2014, **600**, 60-66.
11 T. Gholami, N. Mir, M. Masjedi-Arani, E. Noori and M. Salavati-Niasari, *Mater. Sci. Semicond. Process.*, 2014, **22**, 101-108.
12 S. Middlemas, Z. Z. Fang and P. Fan, *Hydrometallurgy*, 2013, **131-132**, 107-113.
13 D. H. Wu, H. You, D. R. Jin and X. C. Li, *J. Photochem. Photobiol., A*, 2011, **217**, 177-183.
14 J. F. Lei, X. P. Li, W. S. Li, F. Q. Sun, D. S. Lu and J. Yi, *Int. J. Hydrogen Energy*, 2011, **36**, 8167-8172.
15 Z. Wang, Z. M. Ni, D. R. Qiu, T. Y. Chen, G. Y. Tao and P. Y. Yang, *J. Anal. At. Spectrom*., 2004, **19**, 273-276.
16 Z. Wang, T. Y. Tian, G. Y. Tao and P. Y. Yang, *Spectrosc Spect Anal*, 2005, **25**, 556-559.
17 M. Aramendia, M. Resano and F. Vanhaecke, *J. Anal. At. Spectrom*., 2009, **24**, 41-50.
18 G. Q. Xiang, B. Hu, Z. C. Jiang and C. Q. Gong, *J. Mass Spectrom*., 2006, **41**, 1378-1385.
19 J. A. C. Broekaert, *Nature*, 2008, **455**, 1185–1186.
20 M. R. Webb and G. M. Hieftje, *Anal. Chem*., 2009, **81**, 862-867.
21 N. Jakubowski, R. Dorka, E. Steers and A. Tempez, *J. Anal. At. Spectrom*., 2007, **22**, 722– 735.
22 S. L. Lui, Y. Godwal, M. T. Taschuk, Y. Y. Tsui and R. Fedosejevs, *Anal. Chem*., 2008, **80**, 1995 – 2000.
23 S. Weagant and V. Karanassios, *Anal. Bioanal. Chem*., 2009, **395**, 577– 589.
24 D. Staack, A. Fridman, A. Gutsol, Y. Gogotsi and G. Friedman, *Angew. Chem., Int. Ed.* , 2008, **47**, 8020 – 8024.

25 M. Micle, K. Kunze, G. Musa, J. Franzke and U. K. Niemax, *Spectrochim. Acta, Part B*, 2001, **56**, 37 –43.
26 R. K. Marcus and W. C. Davis, *Anal. Chem.*, 2001, **73**, 2903 – 2910.
27 J. C. T. Eijkel, H. Stoeri and A. Manz, *Anal. Chem*., 1999, **71**, 2600–2606.
28 W. C. Davis and R. K. Marcus, *Spectrochim. Acta, Part B*, 2002, **57**, 1473 –1486.
29 G. Jenkins, J. Franzke and A. Manz, *Lab Chip* , 2005, **5**, 711– 718.
30 A. Kitano, A. Iiduka, T. Yamamoto, Y. Ukita, E. Tamiya and Y. Takamura, *Anal. Chem*., 2011, **83**, 9424 – 9430.
31 M. Miclea, K. Kunze, J. Franzke and K. Niemax, *Spectrochim. Acta, Part B,* 2002, **57**, 1585 – 1592.
32 J. Wu, J. Yu, J. Li, J. Wang and Y. Ying, *Spectrochim. Acta, Part B*, 2007, **62**, 1269 – 1272.
33 R. Manjusha, M. A. Reddy, R. Shekhar and S. Jaikumar, *J. Anal. At. Spectrom*., 2013, **28**, 1932-1939.
34 T. Cserfalvi, P. Mezei and P. Apai, *J. Phys. D: Appl. Phys.*, 1993, **26**, 2184 –2188.
35 T. Cserfalvi and P. Mezei, *J. Anal. At. Spectrom*., 1994, **9**, 345– 349.
36 H. J. Kim, J. H. Lee, M. Y. Kim, T. Cserfalvi and P. Mezei, *Spectrochim. Acta, Part B*, 2000, **55**, 823– 831.
37 T. Cserfalvi and P. Mezei, *J. Anal. At. Spectrom*. , 2003, **18**, 596– 602.
38 P. Mezei and T. Cserfalvi, *J. Phys. D: Appl. Phys*. , 2006, **39**, 2534–2539.
39 W. C. Davis and R. K. Marcus, *J. Anal. At. Spectrom*. , 2001, **16**, 931 – 937.
40 V. V. Yagov and M. L. Gentsina, *J. Anal. Chem*. , 2004, **59**, 64 – 70.
41 V. V. Yagov, M. L. Getsina and B. K. Zuev, *J. Anal. Chem*., 2004, **59**, 1037 – 1041.
42 C. G. Wilson and Y. B. Gianchandani, *IEEE Trans. Electron Devices*, 2002, **49**, 2317 – 2322.
43 M. R. Webb, F. J. Andrade, G. Gamez, R. McCrindle and G. M. Hieftje, *J. Anal. At. Spectrom*. , 2005, **20**, 1218– 1225.
44 M. R. Webb, F. J. Andrade and G. M. Hieftje*, Anal. Chem*., 2007, **79**, 7899 – 7905.
45 M. R. Webb, F. J. Andrade and G. M. Hieftje, *Anal. Chem*., 2007, **79**, 7807 – 7812.
46 M. R. Webb, F. J. Andrade and G. M. Hieftje, *J. Anal. At. Spectrom.*, 2007, **22**, 766–774.
47 P. Mezei, T. Cserfalvi and M. Janossy, *J. Anal. At. Spectrom.*, 1997, **12**, 1203–1208.
48 Y. S. Part, S. H. Ku, S. H. Hong, H. J. Kim and E. H. Piepmeier, *Spectrochim. Acta, Part B*, 1998, **53**, 1167–1179.
49 T. Cserfalvi, P. Mezei and P. Apai, *J. Phys. D: Appl. Phys.*, 1993, **26**, 2184–2188.
50 T. Cserfalvi and P. Mezei, *Fresenius' J. Anal. Chem*., 1996, **355**, 813–819.
51 P. Mezei, T. Cserfalvi and L. Csillag, *J. Phys. D: Appl. Phys.*, 2005, **38**, 2804–2811.
52 P. Mezei, T. Cserfalvi, M. Janossy, K. Szocs and H. J. Kim, *J. Phys. D: Appl. Phys.*, 1998, **31**, 2818–2825.
53 A. M. Mottaleb, W. Young-Ah and K. Hyo-Jin, *Microchem. J.*, 2001,**69**, 219–230.
54 R. Shekhar, D. Karunasagar, M. Ranjit and J. Arunachalam, *Anal. Chem.*, 2009, **81**, 8157–8166.
55 Z. Wang, A. J. Schwartz, S. J. Ray and G. M. Hieftje, *J. Anal. At. Spectrom*. , 2013, **28**, 234–240.
56 Z. Zhang, Z. Wang, Q. Li, H. J. Zou, Y. Shi, *Talanta,* 2014, **119**, 613–619.
57 T. A. Doroski, A. M. King, M. P. Fritz and M. R. Webb, *J. Anal. At. Spectrom*. , 2013, **28**, 1090–1095.
58 K. Greda, P. Jamroz and P. Pohl, *Talanta*, 2013, **108**, 74-82.
59 Hill, S. J.; Fisher, A.; Foulkes, M. In *Inductively Coupled Plasma Spectrometry and Its Applications*, 2nd ed.; Hill, S. J., Ed.; Blackwell Publishing Ltd.:Oxford, 2007; pp 61-67.
60 Q. Xiao, Z. L. Zhu, H. T. Zheng, H. Y. He, C. Y. Huang and S. D. Hu, *Talanta*, 2013, **106**, 144-149.
61 T. A. Doroski and M. R. Webb, *Spectrochim. Acta, Part B*, 2013, **88**, 40-45.
62 A. J. Schwartz, S. J. Ray, E. Elish, A. P. Storey, A. A. Rubinshtein, G. C. Y. Chan, K. P. Pfeuffer and G. M. Hieftje, *Talanta*, 2012, **102**, 26-33.